

PCCP

Accepted Manuscript



This is an *Accepted Manuscript*, which has been through the Royal Society of Chemistry peer review process and has been accepted for publication.

Accepted Manuscripts are published online shortly after acceptance, before technical editing, formatting and proof reading. Using this free service, authors can make their results available to the community, in citable form, before we publish the edited article. We will replace this *Accepted Manuscript* with the edited and formatted *Advance Article* as soon as it is available.

You can find more information about *Accepted Manuscripts* in the [Information for Authors](#).

Please note that technical editing may introduce minor changes to the text and/or graphics, which may alter content. The journal's standard [Terms & Conditions](#) and the [Ethical guidelines](#) still apply. In no event shall the Royal Society of Chemistry be held responsible for any errors or omissions in this *Accepted Manuscript* or any consequences arising from the use of any information it contains.

Dissolution of cellulose in ionic liquids: an *ab-initio* molecular dynamics simulation study

Rajdeep Singh Payal and Sundaram Balasubramanian *

Received Xth XXXXXXXXXXXX 20XX, Accepted Xth XXXXXXXXXXXX 20XX

First published on the web Xth XXXXXXXXXXXX 200X

DOI: 10.1039/b000000x

Abstract

Interactions determining the dissolution of a monomer of β -cellulose, i.e., cellobiose in a room temperature ionic liquid, [Emim][OAc] have been studied using *ab-initio* molecular dynamics simulations. Although anions are the predominant species in the first coordination shell of cellobiose, cations too are present to a minor extent around it. Presence of small concentration of water in the solution does not significantly alter the nature of the coordination environment of cellobiose. All intra-molecular hydrogen bonds of anti-syn cellobiose are replaced by inter-molecular hydrogen bonds formed with the anions, whereas the anti-anti conformer retains an intramolecular hydrogen bond.

1 Introduction

The depletion of fossil fuels and the increasing need for energy sources is an issue of paramount importance. Among many alternatives, biomass is a promising candidate. It is most abundant in the form of lignocellulosic matter present in wood or plant biomass. Major components of lignocellulosic biomass are cellulose (40-50%), hemicellulose (20-30%) and lignin (20-30%).¹ Notwithstanding its abundance and utility, the conversion of biomass to biofuel is a rather difficult process. One of the main hurdles in this conversion is its dissolution. Biomass is reluctant to dissolve in conventional organic solvents and requires harsh conditions of pressure and temperature.² Furthermore, traditional solvents for biomass have been associated with issues such as toxicity, volatility etc.

Rogers and coworkers³ pioneered the dissolution of cellulose in ionic liquids (ILs) under mild conditions, without any pretreatment and overcame these challenges. They were also able to regenerate cellulose with addition of water and other common solvents. Ionic liquids are salts that are liquid at room temperature.^{4,5} Since their early work, significant progress has been made in the dissolution of biomass in ionic liquids. Some of the recent studies show that even wood can be directly dissolved in ionic liquids without any pretreatment.^{6,7,8} Researchers have employed a variety of experimental techniques to investigate the dissolution mechanism of cellulose in ILs. Nuclear magnetic resonance (NMR) studies performed by Moyna and coworkers⁹ revealed that hydrogen-bonding interaction between the hydroxyl group of cellulose and the anion of ILs was responsible for

the dissolution of cellulose in ILs and that the cation plays a negligible role. Ludwig and coworkers did a systematic study of dissolution of polyols in different salt solution and ILs.¹⁰ Shift in the OH frequency was used to determine the ability of any solvent to dissolve the polyols. Molecular dynamics (MD) simulations carried out by Youngs et al^{11,12} suggested a similar mechanism. Seddon and coworkers¹³ used ILs to assist the acid-catalysed hydrolysis of lignocellulosic biomass. Motivated by the work of Rogers and coworkers³, many researchers have employed ILs to dissolve other biomolecules. Silk fibroin¹⁴, starch and Zein protein¹⁵, hemicellulose¹⁶, lignin¹⁷, chitin and chitosan¹⁸ etc. have also been dissolved in ILs.

Over time, newer ionic liquids to improve the dissolution of cellulose have been identified.^{19,20,21,22,23} Experimental studies suggest that ILs with imidazolium cation and acetate anion are the best solvents for cellulose. [C₄mim][CH₃COO] can dissolve 15 - 20 % of biomass.^{19,20} Although it is now well known that ILs currently serve as the best solvents for cellulose dissolution, yet the role of cation in this process is under debate. A recent NMR study by Zhang et al²⁴ suggests that both cation and anion form hydrogen bonds with cellulose. In our earlier work²⁵, we attempted to explain the dissolution mechanism of cellulose and hemicellulose in ILs using density functional theory applied to the clusters. It was shown that cations can indeed form weak hydrogen bonds with the hydroxyl groups of cellulose and hemicellulose.

The mechanism of dissolution has been investigated by many researchers using various computational techniques. Bergenstr hle et al²⁶ carried out force field based MD simulations to understand the insolubility of cellulose in

aqueous solutions. Singh and coworkers²⁷ used MD simulations to study the dissolution mechanism of cellulose in [C₂mim][OAc]. They reported that the strong hydrogen bonding between the anion and cellobiose was a major factor in dissolution. They also reported the interaction of a few cations with cellobiose. In particular, they observed a change in the conformation of cellulose with respect to the $\beta(1-4)$ linkage when it was dissolved in the IL. Zhao et al^{28,29} carried out systematic MD simulations to understand the effect of the structure of cation and anion on the dissolution of cellobiose in ILs. Cations with less steric hindrance showed a better dissolution capability. In the case of anions, apart from steric hindrance, a high electronegativity and absence of electron withdrawing groups were shown to aid cellulose dissolution. Recently, Rabideau et al³⁰ carried out atomistic MD simulations to study the dissolution of cellulose bundles in ILs. They too observed that ILs weaken the intra- and intermolecular hydrogen bonding between the cellobiose units, resulting in their dissolution. Quantum chemical calculations have also been employed to understand the interaction of cations and anions with cellulose. Janesko³¹ employed dispersion corrected density functional theory (DFT) to understand the interaction between one ion pair of IL and cellulose. They found that the cellulose unit mainly interacts with the anion (Cl⁻ in their case). Guo et al^{32,33} employed DFT calculations to probe the effect of cation and anion structure on interaction with cellulose. They too reported that the dissolution of cellulose in ILs will have contributions from both cation and anion. Pincu and Gerber have recently carried out ab-initio molecular dynamics (AIMD) simulations of β -cellobiose conformer in pure water and examined differences in the solvation of the two conformers.³⁴

While both gas phase quantum chemical studies as well as force field based MD simulations have been employed to understand the dissolution mechanism of cellobiose in IL, to our knowledge no AIMD simulations have been carried out so far. AIMD simulations have the advantage of both configurational sampling intrinsic to a liquid phase and a quantum chemical framework within which it is realised.^{35, 36, 37, 38, 39, 40} We report results of such simulations here. Ionic liquids, particularly in conditions employed to dissolve biomass are rarely devoid of water. Thus, we have also examined the effect of water concentration in the IL on the solvation of the cellulosic unit.

2 Details of Simulation

As we are interested in examining the microscopic interactions between cellulose and ionic liquid, one monomer unit of cellulose, i.e., cellobiose was considered as the solute. Initial geometries of the structural unit and of the cation and anion

were constructed using GaussView⁴¹. These were later optimized independently in gas phase at B3LYP/6-311++(g,d) level of theory, using the Gaussian 09 software package⁴¹. Two lowest energy conformers for cellobiose and the lowest energy structure of the ions were taken for further calculations. The conformers of cellobiose were either anti - anti or anti - syn, as determined by the torsional state of the two CH₂OH groups (Figure 1). For each of these conformers, two different sets of simulation were carried out. In the first, cellobiose was solvated in pure IL (with 30 ion pairs of IL only). In addition, a simulation containing cellobiose dissolved in 30 ion pairs of IL along with 5 water molecules was also carried out. While the former system consisted of 825 atoms and 2176 valence electrons, the latter involved 840 atoms and 2216 valence electrons, making these simulations rather computationally challenging. Prior experimental studies have suggested the first and second solvation shells of cellobiose to contain 7 and 19 ion pairs respectively²⁴ and thus these system sizes, although small, are not unreasonable.

The system was initially equilibrated using classical MD simulations during which the ionic liquid was described using the force field of Senapati et al⁴². Water was described using the SPC/E model⁴³. Gas phase ESP charges for atoms on cellobiose were calculated through Gaussian-09⁴¹ and the same were used in these classical MD simulations. The initial configuration of solvent molecules in each system was generated using Packmol.⁴⁴ The system was energy minimized prior to a short MD run under constant NVT conditions of 500 ps. Subsequently, the systems were studied under constant NPT conditions for 15 ns. This was followed by a constant NVT run for 16 ns whose final configuration constituted the initial configuration for the AIMD run. Box lengths for the systems containing anti-anti or anti-syn conformer soaked in pure IL were 19.8802 Å and 19.8806 Å respectively. For the IL+5H₂O systems, it was 19.9796 Å for the anti-anti conformer and 20.1040 Å for the anti-syn one. All classical MD simulations were carried out using the LAMMPS⁴⁵ software package.

AIMD simulations were performed using the CP2K/Quickstep code.⁴⁶ Double zeta valence polarization (DZVP) basis with Goedecker, Teter and Hutter (GTH) pseudopotentials were used. The BLYP⁴⁷ exchange-correlation functional was employed. Dispersion corrections at the D2 level⁴⁸ were also included. Simulations were carried out in the NVT ensemble at 300 K using a Nosé-Hoover chain thermostat.⁴⁹ Equations of motion were integrated with 0.5 fs timestep. Three dimensional periodic boundary conditions were employed in order to mimic a bulk system. Electronic orbitals were expanded in a Gaussian basis set. The electron density was expanded in plane wave basis set with energy cut off of 280 Ry. All the systems were studied for 35 ps. All the analyses were carried out on the

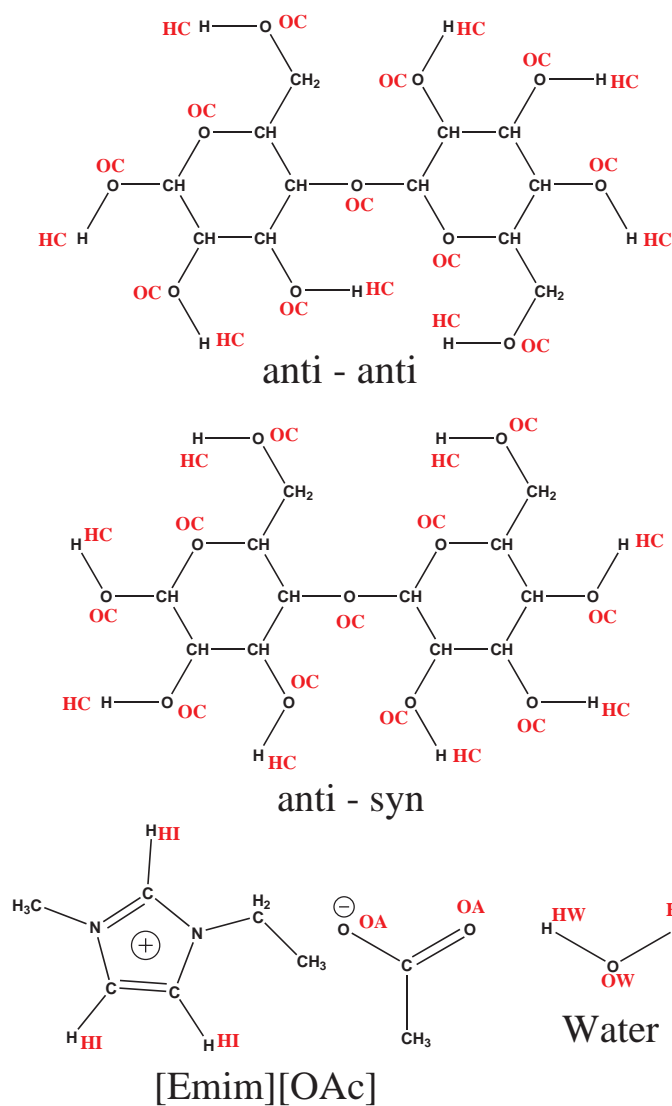


Fig. 1 Schematic of the two cellobiose conformers, ions of ionic liquid and water molecule, showing different atom types used in the discussion.

last 25 ps of the AIMD trajectory using home grown codes written in FORTRAN 90.

MD trajectories were visualized and spatial density maps were created using VMD.⁵⁰

3 Results and Discussion

The structural properties of a liquid system can be well studied through the radial distribution function, $g(r)$. Figure 2(a) shows the $g(r)$ between the three ring hydrogen atoms of the cation (HIs) and the oxygen (OC) atom of cellobiose. All these pair correlation functions exhibit a first peak at around 2.7 Å; on rare occasions, the ring hydrogen of the cation approaches cellobiose to distances less than 2 Å indicating the likely formation of a weak cation-cellobiose hydrogen bond. Addition of water decreases the height of the first peak in the anti-anti case; thus, water could partially displace the cations in the first coordination shell of cellobiose. Figure 2(b) shows the $g(r)$ between oxygen (OA) of anion and hydroxyl hydrogen (HC) of cellobiose. The sharp peak at 1.6 Å in all the $g(r)$ s indicates the formation of strong hydrogen bonds. Also the peak height changes negligibly upon addition of water, implying that anions surrounding the cellobiose unit are more or less unaffected by the presence of water molecules.

This behavior is evident from the running coordination number (Figure 4). The running coordination number of cation HIs around OC of cellobiose is insignificant till 2 Å. However, in the corresponding distance range, that of anion OAs around HC of cellobiose varies between 0.70 to 0.85. Thus, each of the hydroxyl hydrogen of cellobiose is surrounded by 0.75 anion oxygens. Given that there are eight HC atoms in cellobiose, we can conclude the presence of around six to seven anions hydrogen bonded to cellobiose, in its first coordination shell. This observation can be further supported by the radial distribution function between the HC of cellobiose and carboxylate carbon of anion (See Figure S1). At the first coordination minimum (3.5 Å), the coordination number is around 0.85. As there are 8 HCs in cellobiose, one can say that nearly 7 anions are hydrogen bonded to it. The acetate anion possesses two carboxylate oxygen atoms (OA). Either of them can form hydrogen bond with hydroxyl hydrogen (HC) of cellobiose. However, we observe that only one of the two OAs hydrogen bonds with HC. The other OA atom is hydrogen bonded with the acidic proton of the cation (see Figure 3). For the case of cellobiose-cation, the first coordination shell extends up to 3.25 Å and the number of cations varies between 0.50 to 1.0; however, the coordination number at 2.5 Å is only 0.4. Thus, within this distance from cellobiose, nearly six to seven anions are hydrogen bonded and around three to four cations are present. This observation is in reasonable agreement with the earlier NMR study of Zhang et al.²⁴, where they suggested the first coordination

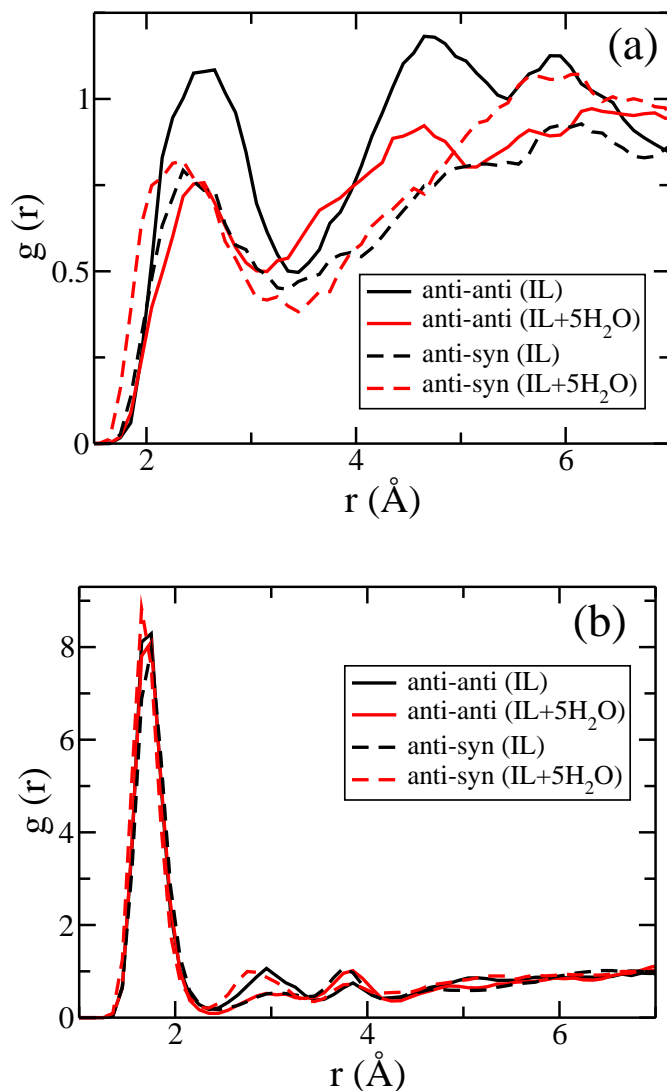


Fig. 2 Radial distribution function between (a) OC of cellobiose and HI of cation and (b) HC of cellobiose and OA of anion.

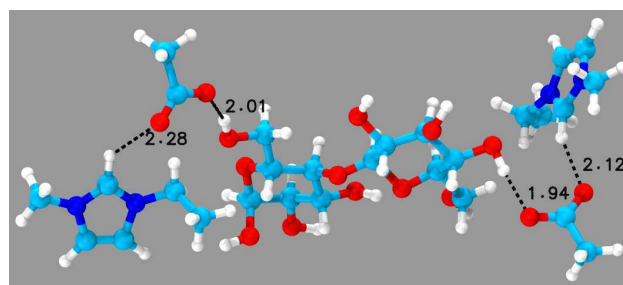


Fig. 3 Snapshot from simulation exhibiting the neighbourhood of cellobiose in ionic liquid. Only one of the OA atom of acetate anion is hydrogen bonded with HC of cellobiose. The other OA atom is hydrogen bonded to HI of the cation. Only two anions present around cellobiose are shown for the sake of clarity.

shell of cellobiose to consist of 7 ion pairs. Since anions are seen to be closer to the cellobiose units, it can be concluded that they form stronger hydrogen bonds and play the primary role in its dissolution which is in agreement with earlier experimental^{9, 11} and simulation studies.²⁷

While the role of anions in the dissolution mechanism is widely accepted, that of the cations needs to be understood better. Plots of both radial distribution function and running coordination number suggest that cations can approach cellobiose close enough such that their HIs can form weak hydrogen bonds with the OC atoms of cellobiose. The cation-cellobiose hydrogen bonds are considerably weaker as compared to those formed by the anions. These results are in agreement with our previous cluster calculations²⁵, in the sense that both cation and anion are found to interact favorably with cellobiose. Further, these observations are in agreement with the NMR spectroscopic studies of Zhang et al.²⁴ Thus, although the cation has only a secondary role to play in the dissolution mechanism, its effect cannot be neglected, a conclusion drawn through MD simulations recently reported by Zhao et al.²⁸ Further, the shortest distance of approach for both the cation and the anion to cellobiose is independent of the amount of water present, although the peak height of the cellobiose-ion $g(r)$ decreases with increasing water concentration. Similar effect of cation on dissolution of CO₂ in ILs was observed by Kirchner and coworkers.⁵¹ In case of CO₂ dissolution also anion plays the major role. Examination of the first solvation shell for the anti-anti conformer of cellobiose shows that all but one of its intramolecular hydrogen bonds are replaced by intermolecular hydrogen bonds between cellobiose and ions of IL (see Figure S2 in Supporting information). Interestingly, the unbroken intramolecular hydrogen bond present in the anti-anti conformer is found to be broken in the anti-syn case (see Figure S3 in Supporting Information). Through DFT calculations of clusters, we had reported earlier²⁵ that the

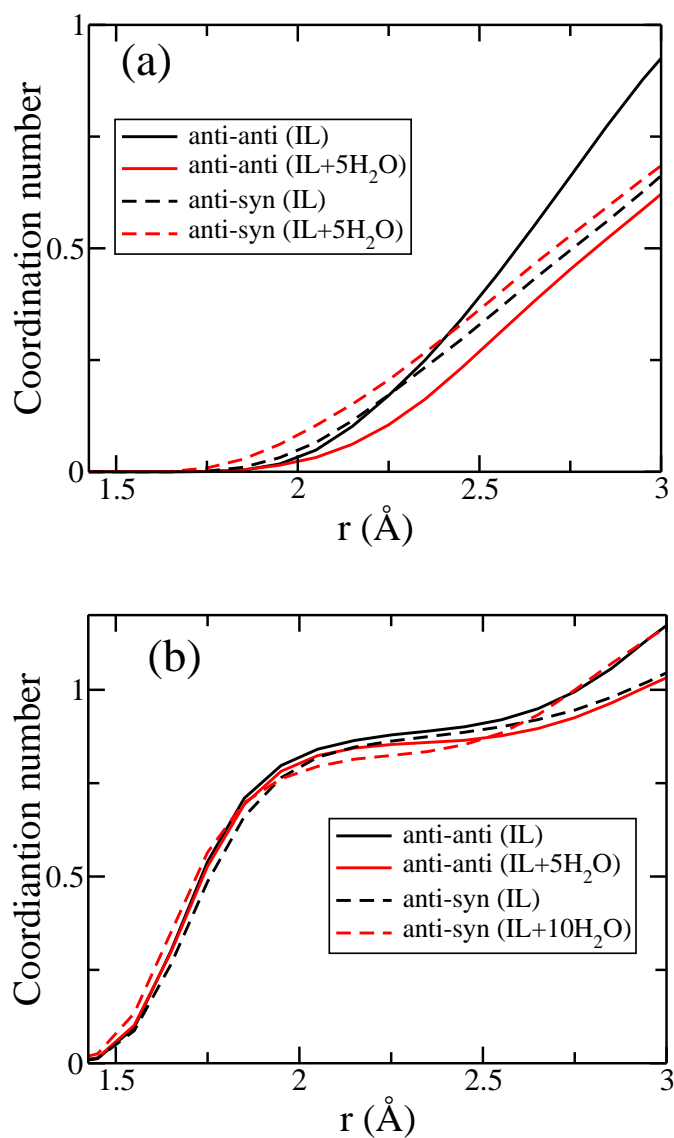


Fig. 4 Running coordination number between (a) OC atom of cellobiose and HI of cation and (b) HC of cellobiose and OA of anion.

anti-anti conformer, which is the most stable in gas phase, becomes less stable than the anti-syn one in the presence of explicit ions of IL. The results reported here on the absence of an intramolecular hydrogen bond in the anti-syn conformer confirms our earlier observations. This structural detail is observed in the systems studied with water as well.

Figures 5 and 6 show the spatial density map of the three ring hydrogens of cation (HI) and of oxygens of the anion (OA) around the two cellobiose conformers. Both anion and the cation are present in the first coordination shell of cellobiose. The isosurface value used for the cation in the figures is an order of magnitude larger than that for the anion. Despite its higher isosurface value, the cation map is much more dispersed than the corresponding one for the anion. Anions exhibit very specific binding as seen from their relatively narrow spatial distribution. The bulky nature of the cations may impose steric hindrance and does not permit them to approach closer to the hydroxyl sites of cellobiose. In addition, the larger volume over which the positive charge is distributed on the cation could also be a reason for its weaker binding to cellobiose. In the case of the anti-anti conformer, anions are absent near one of the hydroxyl hydrogens as the latter forms an intramolecular hydrogen bond which is intact over the entire duration of the simulation (see Figure S2 in Supporting Information). In fact, the hydrogen bond that this hydrogen atom participates in, exhibits an interesting behavior. As shown in Figure 7(a), it can form a hydrogen bond with either O1 (ring oxygen) or with O2 (CH₂OH). Shown in Figure 7(b) is the distance of this hydrogen from these two sites as a function of time in the case of cellobiose dissolved in pure IL. Over the duration of the AIMD trajectory, we find that this hydrogen forms a hydrogen bond between these two sites in the ratio of approximately 4:1, i.e., the ring oxygen site (O1) is more preferred than the CH₂OH oxygen (O2). There also exists a transient state where the intramolecular hydrogen bond is replaced by the intermolecular hydrogen bond (7(c)). In the anti-syn conformer, this intramolecular hydrogen bond was never observed and is replaced by an intermolecular one – the hydrogen atom h-bonds with OA of the anion (see Figure S3 in Supporting Information).

Figure 8 is a snapshot from the AIMD simulation displaying the cations and anions in the vicinity of the cellobiose unit. Most of the HC atoms of cellobiose form hydrogen bonds with one of the OA atoms. The other OA atoms of the anion are seen to form a hydrogen bond with the HI of cation. In most cases of hydrogen bond between the anion and the cation, the most acidic ring hydrogen is the atom which is involved. In the vicinity of cellobiose, some cations are seen not to form hydrogen bond with it. However, they are involved in hydrogen bonds with anions.

Figures 9 and S4 (Supporting information) compare the pair

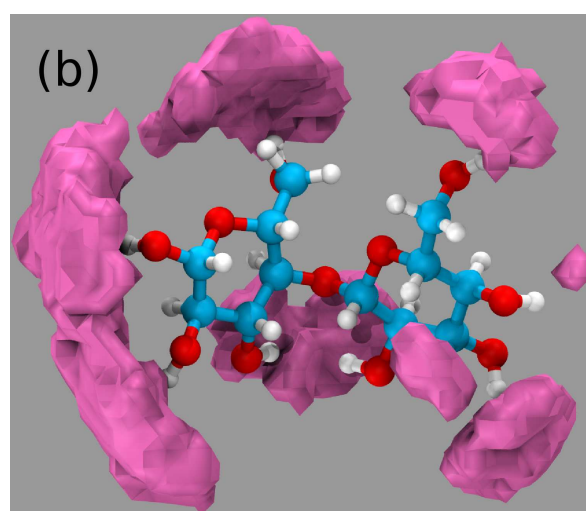
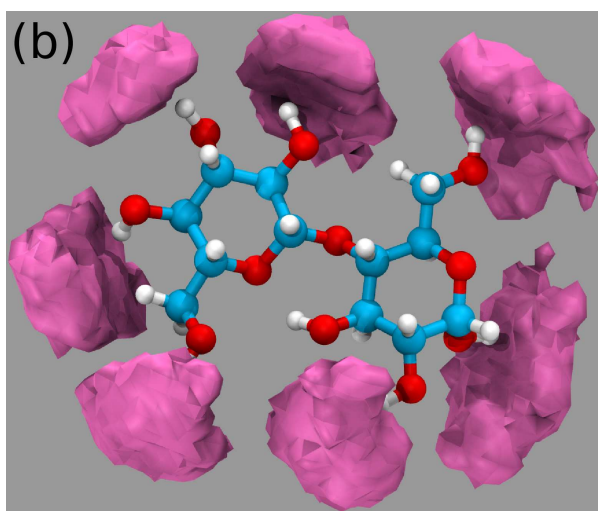
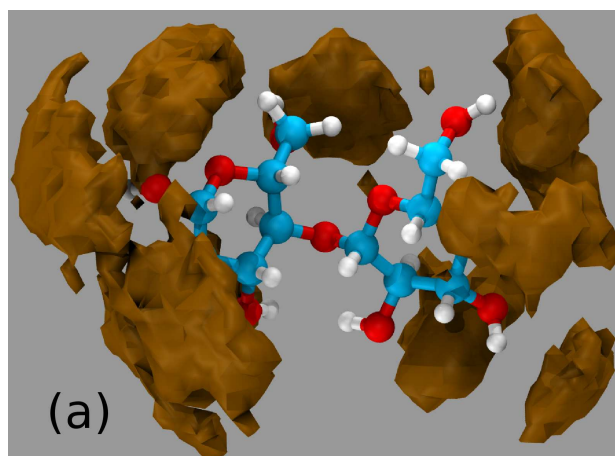
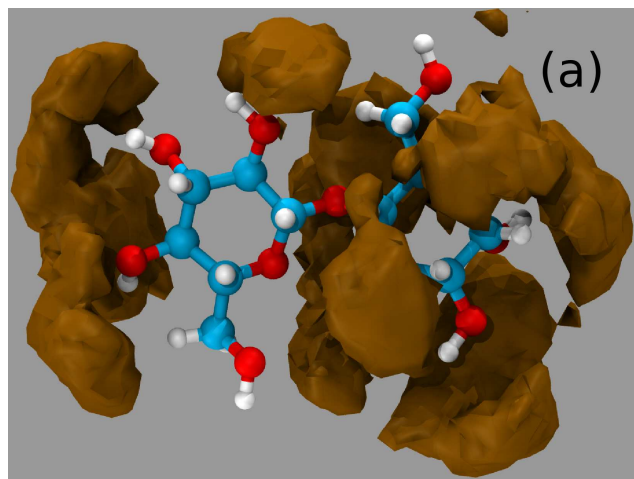


Fig. 5 Spatial distribution of (a) cation's ring hydrogen and of (b) anion's oxygen around cellobiose in anti-anti conformation. Isosurface values are 0.01 \AA^{-3} and 0.001 \AA^{-3} respectively. Carbon : Cyan, Oxygen : Red and Hydrogen : White.

Fig. 6 Spatial distribution of (a) cation's ring hydrogen and of (b) anion's oxygen around cellobiose in anti-syn conformation. Isosurface values and colour scheme are same as in Figure 5.

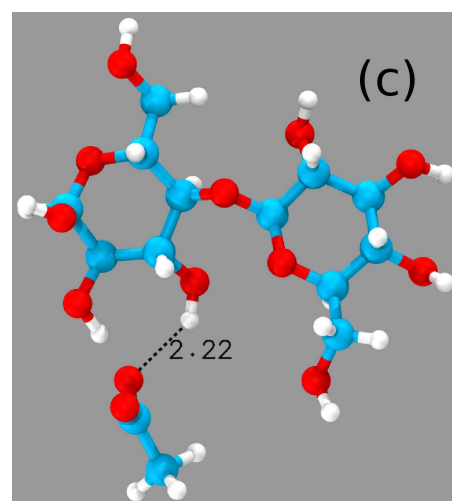
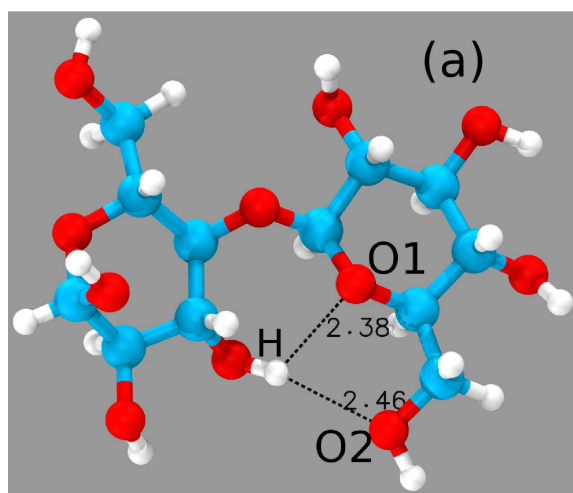


Fig. 7 (a) Snapshot of cellobiose taken from the AIMD trajectory. O1 and O2 are two possible hydrogen bonding sites for H atom of cellobiose in its anti - anti conformation. (b) distance of H from O1 and O2 during the AIMD trajectory and (c) a transient state, where such intramolecular hydrogen bond(s) are replaced by one intermolecular hydrogen bond with the anion. Colour scheme is the same as in earlier figures. Distances are in Å units.

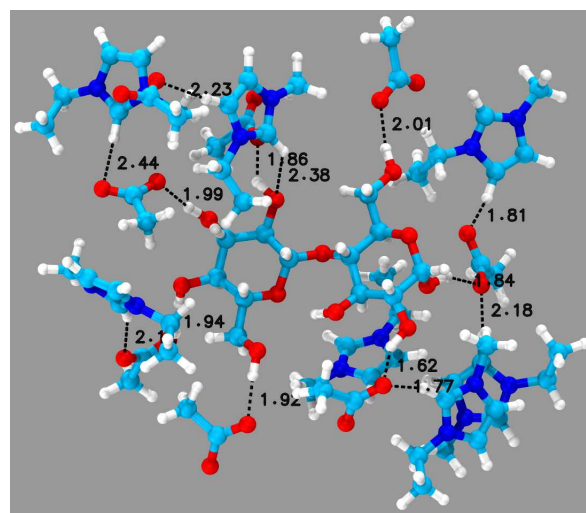
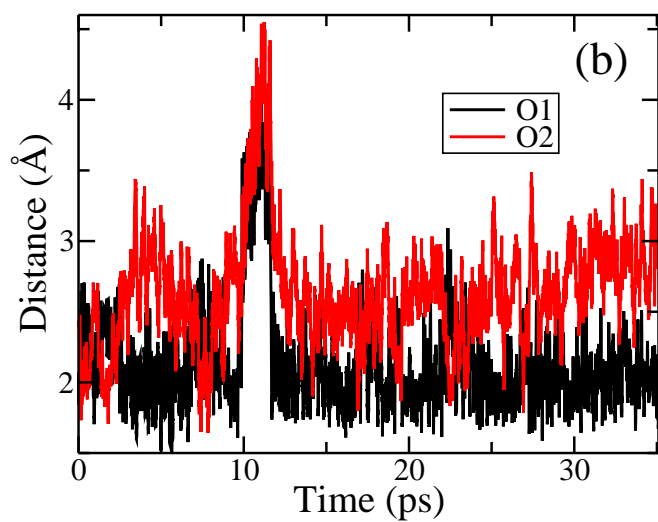


Fig. 8 Environment around cellobiose solvated in ionic liquid. Colour scheme same as in earlier figures, Nitrogen : Blue.

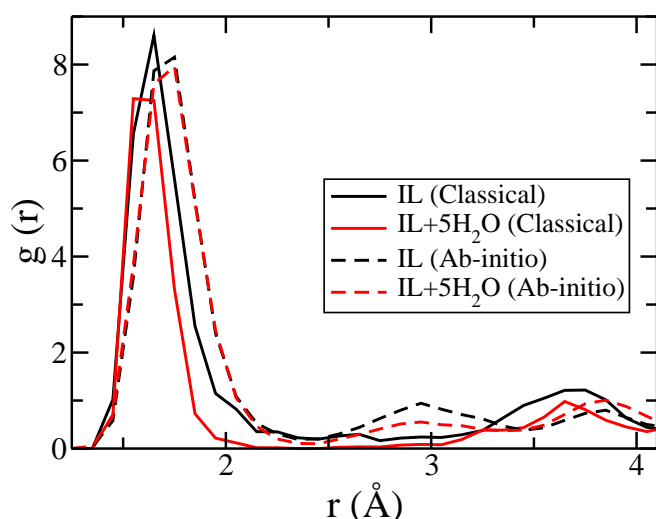


Fig. 9 Comparison of OA-HC RDFs obtained from classical and ab-initio MD simulations for the anti - anti conformer of cellobiose.

correlation functions between anions and cellobiose obtained from force field based MD (with empirical potentials) and AIMD simulations. The $g(r)$ s between the anion's oxygen and cellobiose's hydroxyl hydrogen are nearly identical as obtained from the two methods. Since this hydrogen bonding is the most dominant interaction between cellobiose and the ions, the current results can also be seen as a validation of the classical force field. However in both the cases, the anion-cellobiose $g(r)$ is shifted to higher distances in AIMD simulations. This observation suggests that the anion may be overbound in classical force field based simulations. Typical force fields of ILs employ a unit charge on the ions although many researchers^{52, 53, 54, 55} advocate a sub-unit charge to account for charge transfer and polarization effects present in the condensed phase. The force field employed herein treats the ions with unit charge and this is likely to have led to the overbinding of anions to cellobiose within the force field description.

Figure S5 (Supporting information) compares various $g(r)$ s of IL-cellobiose and water-cellobiose. The ions approach the cellobiose unit closer than water does. Furthermore, within water, its oxygen atom (OW) is closer to cellobiose than its hydrogen (HW). Thus, water chiefly acts as a hydrogen bond acceptor with cellobiose. However, the effect of water on the two conformers is different. A comparison between the running coordination number of (HI-HW) and (OA-OW) pairs (see Figure S6 in Supporting Information) captures the difference in the nature of interaction of water molecules with the two cellobiose conformers rather well. For both the conformers, the running coordination number of HW around OC is insignificant for distances less than 2.5 Å, while OW

approaches HC up to a distance of 2.0 Å. The latter suggests the occasional formation of a OW-HC hydrogen bond. Figure S5 also demonstrates that water molecules interact differently with each conformer. Water molecules are able to approach closer to the anti-anti conformer as compared to the anti-syn conformer. The effect of cellobiose geometry on its interaction with pure water has already been studied by Pincu and Gerber³⁴ using AIMD simulations. They too observed the two conformers of cellobiose to interact differently with water and concluded that water molecules are able to better solvate the anti-anti conformer than the anti-syn one. The presence of water was not able to alter the nature of the solvation shell of cellobiose significantly. This may be due to the small concentration of water studied here.

During the AIMD run, no conformational transition was observed in the cellobiose; the anti-anti and anti-syn conformers retained their respective torsional angles for the bond between the two pentose rings (See Figure S7 in Supporting Information). The torsional angle about the $\beta(1-4)$ linkage varied between 40 and 80°, in agreement with an earlier MD simulations of Singh et al.²⁷ Furthermore, it was observed that the hydrogen bonds formed by cellobiose with the cation, anion or any water molecule were intact during the entire duration of the AIMD simulation.

4 Conclusions

The dissolution of cellulose in ILs depends on the breaking of the strong, inter and intra-molecular hydrogen bonding network present in cellulose. ILs are able to disrupt this hydrogen bonding network more efficiently. The anions of IL play the major role in the dissolution mechanism. They form strong hydrogen bonds with hydroxyl hydrogens of cellobiose, in either of its conformers (anti-anti or anti-syn). However, the role of cation in the solvation of cellobiose cannot be completely ignored. Strong electrostatic interactions between the cation and the anion necessitate that the cation be proximal to the anion. Thus, a few cations are indeed present in the first coordination shell of cellobiose. They too form hydrogen bonds with the cellobiose unit, albeit weaker ones than what the anions do. The coordination offered by the ions of IL to the anti-anti and anti-syn conformer of cellobiose are different. Thus the conformation of cellobiose will play a crucial role in its dissolution in the ionic liquid. The addition of a small quantity of water does not significantly alter the local environment of the cellobiose which continues to be coordinated primarily by the ions.

5 Acknowledgement

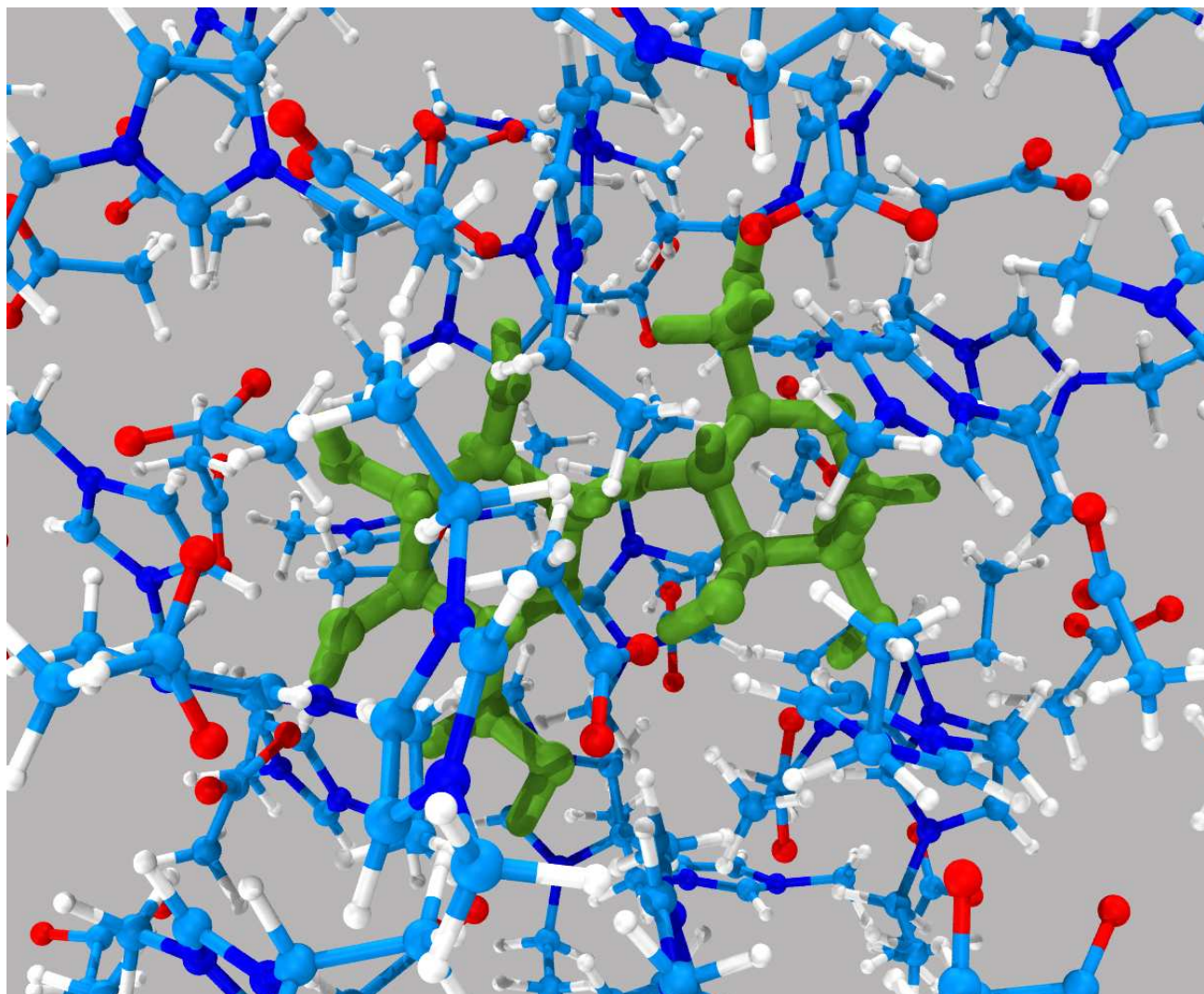
RSP thanks CSIR for a Senior Research Fellowship. We thank DST for support. SB thanks Sheikh Saqr Laboratory for a senior fellowship.

References

- 1 B. C. Saha, *J. Ind. Microbiology and biotech.*, 2003, **30**, 279–291.
- 2 T. Nishino, I. Matsuda and K. Hirao, *Macromolecules*, 2004, **37**, 7683–7687.
- 3 R. P. Swatloski, S. K. Spear, J. D. Holbrey and R. D. Rogers, *J. Am. Chem. Soc.*, 2002, **124**, 4974–4975.
- 4 R. D. Rogers and K. R. Seddon, *Science*, 2003, **302**, 792–793.
- 5 P. Hunt, *Mol. Sim.*, 2006, **32**, 1–10.
- 6 D. A. Fort, R. C. Remsing, R. P. Swatloski, P. Moyna, G. Moyna and R. D. Rogers, *Green Chem.*, 2007, **9**, 63–69.
- 7 N. Sun, M. Rahman, Y. Qin, M. L. Maxim, H. Rodriguez and R. D. Rogers, *Green Chem.*, 2009, **11**, 646–655.
- 8 A. Brandt, J. P. Hallett, D. J. Leak, R. J. Murphy and T. Welton, *Green Chem.*, 2010, **12**, 672–679.
- 9 R. C. Remsing, R. P. Swatloski, R. D. Rogers and G. Moyna, *Chem. Commun.*, 2006, 1271–1273.
- 10 Z. Papanayan, C. Roth, K. Wittler, S. Reimann and R. Ludwig, *ChemPhysChem*, 2013, **14**, 3667–3671.
- 11 T. G. A. Youngs, C. Hardacre and J. D. Holbrey, *J. Phys. Chem.*, 2007, **111**, 13765–13774.
- 12 T. G. Youngs, J. D. Holbrey, M. Deetlefs, M. Nieuwenhuyzen, M. F. Costa Gomes and C. Hardacre, *ChemPhysChem*, 2006, **7**, 2279–2281.
- 13 L. Vanoye, M. Fanselow, J. D. Holbrey, M. P. Atkins and K. R. Seddon, *Green Chem.*, 2009, **11**, 390–396.
- 14 D. M. Phillips, L. F. Drummy, D. G. Conrady, D. M. Fox, R. R. Naik, M. O. Stone, P. C. Trulove, H. C. De Long and R. A. Mantz, *J. Am. Chem. Soc.*, 2004, **126**, 14350–14351.
- 15 A. Biswas, R. Shogren, D. Stevenson, J. Willett and P. K. Bhowmik, *Carbohydrate Polymers*, 2006, **66**, 546–550.
- 16 H. Zhao, G. A. Baker and J. V. Cowins, *Biotechnology Progress*, 2010, **26**, 127–133.
- 17 Y. Pu, N. Jiang and A. J. Ragauskas, *J. Wood Chem. and Technology*, 2007, **27**, 23–33.
- 18 H. Xie, S. Zhang and S. Li, *Green Chem.*, 2006, **8**, 630–633.
- 19 M. Zavrel, D. Bross, M. Funke, J. Bchs and A. C. Spiess, *Bioresource Technology*, 2009, **100**, 2580–2587.
- 20 S. Singh, B. A. Simmons and K. P. Vogel, *Biotechnology and Bioengineering*, 2009, **104**, 68–75.
- 21 Y. Fukaya, A. Sugimoto and H. Ohno, *Biomacromolecules*, 2006, **7**, 3295–3297.
- 22 A. Xu, J. Wang and H. Wang, *Green Chem.*, 2010, **12**, 268–275.
- 23 Y. Fukaya, K. Hayashi, M. Wada and H. Ohno, *Green Chem.*, 2008, **10**, 44–46.
- 24 J. Zhang, H. Zhang, J. Wu, J. Zhang, J. He and J. Xiang, *Phys. Chem. Chem. Phys.*, 2010, **12**, 1941–1947.
- 25 R. S. Payal, R. Bharath, G. Periyasamy and S. Balasubramanian, *J. Phys. Chem. B*, 2012, **116**, 833–840.
- 26 M. Bergensträhle, J. Wohler, M. E. Himmel and J. W. Brady, *Carbohydrate Research*, 2010, **345**, 2060–2066.
- 27 H. Liu, K. L. Sale, B. M. Holmes, B. A. Simmons and S. Singh, *J. Phys. Chem. B*, 2010, **114**, 4293–4301.
- 28 Y. Zhao, X. Liu, J. Wang and S. Zhang, *ChemPhysChem*, 2012, **13**, 3126–3133.
- 29 Y. Zhao, X. Liu, J. Wang and S. Zhang, *Carbohydrate Polymers*, 2013, **94**, 723–730.
- 30 B. D. Rabideau, A. Agarwal and A. E. Ismail, *J. Phys. Chem. B*, 2013, **117**, 3469–3479.
- 31 B. G. Janesko, *Phys. Chem. Chem. Phys.*, 2011, **13**, 11393–11401.
- 32 J. Guo, D. Zhang, C. Duan and C. Liu, *Carbohydrate Research*, 2010, **345**, 2201–2205.
- 33 C. Liu, J. Guo and D. Zhang, *J. Theor. Comput. Chem.*, 2010, **09**, 611–624.
- 34 M. Pincu and R. B. Gerber, *Chem. Phys. Lett.*, 2012, **531**, 52–58.
- 35 R. Iftimie, P. Minary and M. E. Tuckerman, *Proc. Natl. Acad. Sci. USA*, 2005, **102**, 6654–6659.
- 36 D. Marx and J. Hutter, *Modern methods and algorithms of quantum chemistry*, 2000, **1**, 301–449.
- 37 M. Thomas, M. Brehm, R. Fligg, P. Vöhringer and B. Kirchner, *Phys. Chem. Chem. Phys.*, 2013, **15**, 6608–6622.
- 38 C. Spickermann, J. Thar, S. Lehmann, S. Zahn, J. Hunger, R. Buchner, P. Hunt, T. Welton and B. Kirchner, *J. Chem. Phys.*, 2008, **129**, 104505.
- 39 A. D. Boese, A. Chandra, J. M. Martin and D. Marx, *J. Chem. Phys.*, 2003, **119**, 5965–5980.
- 40 D. Chakraborty and A. Chandra, *J. Chem. Phys.*, 2011, **135**, 114510.
- 41 M. J. Frisch, G. W. Trucks, H. B. Schlegel, G. E. Scuseria, M. A. Robb, J. R. Cheeseman, G. Scalmani, V. Barone, B. Mennucci, G. A. Petersson, H. Nakatsuji, M. Caricato, X. Li, H. P. Hratchian, A. F. Izmaylov, J. Bloino, G. Zheng, J. L. Sonnenberg, M. Hada, M. Ehara, K. Toyota, R. Fukuda, J. Hasegawa, M. Ishida, T. Nakajima, Y. Honda, O. Kitao, H. Nakai, T. Vreven, J. A.

- 475 Montgomery, Jr., J. E. Peralta, F. Ogliaro, M. Bearpark,
476 J. J. Heyd, E. Brothers, K. N. Kudin, V. N. Staroverov,
477 R. Kobayashi, J. Normand, K. Raghavachari, A. Rendell,
478 J. C. Burant, S. S. Iyengar, J. Tomasi, M. Cossi, N. Rega,
479 J. M. Millam, M. Klene, J. E. Knox, J. B. Cross,
480 V. Bakken, C. Adamo, J. Jaramillo, R. Gomperts, R. E.
481 Stratmann, O. Yazyev, A. J. Austin, R. Cammi, C. Pomelli,
482 J. W. Ochterski, R. L. Martin, K. Morokuma, V. G.
483 Zakrzewski, G. A. Voth, P. Salvador, J. J. Dannenberg,
484 S. Dapprich, A. D. Daniels, J. P. Farkas, J. B. Foresman, J. V.
485 Ortiz, J. Cioslowski and D. J. Fox, *Gaussian 09 Revision*
486 *D.01*, Gaussian Inc. Wallingford CT 2009.
- 487 42 A. Chandran, K. Prakash and S. Senapati, *Chem. Phys.*,
488 2010, **374**, 46 – 54.
- 489 43 H. J. C. Berendsen, J. R. Grigera and T. P. Straatsma, *J.*
490 *Phys. Chem.*, 1987, **91**, 6269–6271.
- 491 44 L. Martínez, R. Andrade, E. G. Birgin and J. M. Martínez,
492 *J. Comput. Chem.*, 2009, **30**, 2157–2164.
- 493 45 S. Plimpton, *J. Comput. Phys.*, 1995, **117**, 1 – 19.
- 494 46 J. Hutter, M. Iannuzzi, F. Schiffmann and
495 J. VandeVondele, *Wiley Interdisciplinary Reviews:*
496 *Computational Molecular Science*, 2013, 15–25.
- 497 47 A. D. Becke, *Phys. Rev. A*, 1988, **38**, 3098–3100.
- 498 48 S. Grimme, *J. Comput. Chem.*, 2006, **27**, 1787–1799.
- 499 49 G. J. Martyna, M. L. Klein and M. Tuckerman, *J. Chem.*
500 *Phys.*, 1992, **97**, 2635–2643.
- 501 50 W. Humphrey, A. Dalke and K. Schulten, *J. of Mol.*
502 *Graph.*, 1996, **14**, 33–38.
- 503 51 O. Hollóczki, Z. Kelemen, L. Könczöl, D. Szieberth,
504 L. Nyulászi, A. Stark and B. Kirchner, *ChemPhysChem*,
505 2013, **14**, 315–320.
- 506 52 F. Dommert, K. Wendler, R. Berger, L. Delle Site and
507 C. Holm, *ChemPhysChem*, 2012, **13**, 1625–1637.
- 508 53 A. Mondal and S. Balasubramanian, *J. Phys. Chem. B*,
509 2014, **118**, 3409–3422.
- 510 54 I. V. Leontyev and A. A. Stuchebrukhov, *J. Chem. Phys.*,
511 2009, **130**, 085102.
- 512 55 B. L. Bhargava and S. Balasubramanian, *J. Chem. Phys.*,
513 2007, **127**, 114510.

Table of Contents



Dissolution of cellulose in ionic liquid involves breaking of its inter and intra-molecular hydrogen bonding network, as seen through ab initio molecular dynamics simulations.